Cell, Vol. 103, 621–632, November 10, 2000, Copyright ©2000 by Cell Press

Structure of the Molecular Chaperone Prefoldin: Unique Interaction of Multiple Coiled Coil Tentacles with Unfolded Proteins

Ralf Siegert,† Michel R. Leroux,†‡ Clemens Scheufler, F. Ulrich Hartl,* and Ismail Moarefi*
Max-Planck Institut für Biochemie
Am Klopferspitz 18a
D82152 Martinsried
Germany

Summary

Prefoldin (GimC) is a hexameric molecular chaperone complex built from two related classes of subunits and present in all eukaryotes and archaea. Prefoldin interacts with nascent polypeptide chains and, in vitro, can functionally substitute for the Hsp70 chaperone system in stabilizing non-native proteins for subsequent folding in the central cavity of a chaperonin. Here, we present the crystal structure and characterization of the prefoldin hexamer from the archaeum *Methanobacterium thermoautotrophicum*. Prefoldin has the appearance of a jellyfish: its body consists of a double β barrel assembly with six long tentacle-like coiled coils protruding from it. The distal regions of the coiled coils expose hydrophobic patches and are required for multivalent binding of nonnative proteins.

Introduction

Molecular chaperone systems that promote the correct folding of nascent or misfolded proteins in the crowded cellular environment have evolved in all three kingdoms of life. Chaperones typically interact with and stabilize hydrophobic peptide sequences that are ultimately buried in the folded protein but which become exposed transiently during protein synthesis or upon denaturation in conditions of cellular stress. Some chaperone complexes termed chaperonins assist protein folding by providing a cavity in which nonnative polypeptides can be enclosed and thus be protected against intermolecular aggregation. The minimal chaperone machinery found in the known bacterial genomes consists of the nascent chain binding chaperones trigger factor (TF) and Hsp70 (together with its cofactors DnaJ and GrpE) as well as the Group I chaperonin system GroEL/GroES that acts posttranslationally in folding (Hartl, 1996; Sigler et al., 1998; Ellis and Hartl, 1999).

In *Escherichia coli*, the ATP-independent TF and the ATP-regulated DnaK (Hsp70) proteins have partially overlapping but essential functions in stabilizing exposed hydrophobic surfaces of nascent and newly synthesized polypeptides (Deuerling et al., 1999; Teter et al., 1999). In addition, ~10% of newly synthesized bacterial proteins complete their folding in the sequestered environment provided by GroEL/GroES (Horwich et al., 1993; Ewalt et al., 1997; Houry et al., 1999). The eukaryotic Hsp70 chaperone machine also binds nascent chains (Beckmann et al., 1990; Nelson et al., 1992; Eggers et al., 1997; Thulasiraman et al., 1999), and some proteins, including actins and tubulins, depend on the Group II cytosolic chaperonin TRiC (TCP-1 ring Complex; also termed CCT) for folding (Frydman et al., 1992; Gao et al., 1992; Yaffe et al., 1992; Kubota et al., 1995; Siegers et al., 1999).

The archaeal Group II chaperonin (thermosome) is closely related to its eukaryotic homologue TRiC (Gutsche et al., 1999). In contrast, Hsp70 proteins and TF are generally missing from the archaeal kingdom though some archaea have acquired Hsp70, presumably by lateral gene transfer (Gribaldo et al., 1999). However, all archaea contain a homologue of the recently described eukaryotic molecular chaperone prefoldin/GimC (Geissler et al., 1998; Vainberg et al., 1998; Hansen et al., 1999; Siegers et al., 1999), which is absent in bacteria. Archaeal prefoldin has been shown to have ATP-independent chaperone properties similar to that of Hsp70 in a folding pathway with a chaperonin in vitro (Leroux et al., 1999), and may perform Hsp70-like functions in vivo.

The structures and functions of Hsp70 and chaperonins have been extensively reviewed (Hartl, 1996; Bukau and Horwich, 1998; Sigler et al., 1998; Ellis and Hartl, 1999; Fink, 1999). DnaK binds short peptide stretches bearing a core of hydrophobic residues, using a cleft and a lid whose opening and closing is mediated via regulated changes in the ATPase domain of the protein (Zhu et al., 1996; Rüdiger et al., 1997). Group I chaperonins generally form homoheptameric rings stacked back-to-back to yield a cylinder with two central cavities (Langer et al., 1992; Braig et al., 1994; Chen et al., 1994). GroEL binds hydrophobic surfaces exposed in nonnative proteins by way of conserved hydrophobic residues present on the apical domains lining the opening of the cylinder (Braig et al., 1994; Fenton et al., 1994; Hlodan et al., 1995; Chen and Sigler, 1999; Kobayashi et al., 1999). Binding of ATP and the dome-shaped cofactor GroES displaces the bound substrate to the inside of the GroEL cavity, where folding is facilitated by preventing aggregation and perhaps also by unfolding kinetically trapped folding intermediates (Mayhew et al., 1996; Roseman et al., 1996; Weissman et al., 1996; Xu et al., 1997; Coyle et al., 1999; Shtilerman et al., 1999). Group II chaperonins are distantly sequence-related to Group I chaperonins and have a similar overall architecture (Kim et al., 1994). They consist of 8- or 9-membered rings and function independent of a GroES-like capping cofactor. Instead, they apparently rely on α-helical extensions of their apical domains that are thought to mediate the opening and closing of their folding chamber (Klumpp et al., 1997; Ditzel et al., 1998; Llorca et al., 1999; Schoehn et al., 2000).

Little is known about the structure and substrate bind-

*To whom correspondence should be addressed (email: ismail@moarefi.com [I. M.], uhartl@biochem.mpg.de [F. U. H.]).
†These authors contributed equally to the work.
‡Present address: Department of Molecular Biology and Biochemistry, Simon Fraser University, 8888 University Drive, Burnaby, B.C. Canada V5A 1S6.

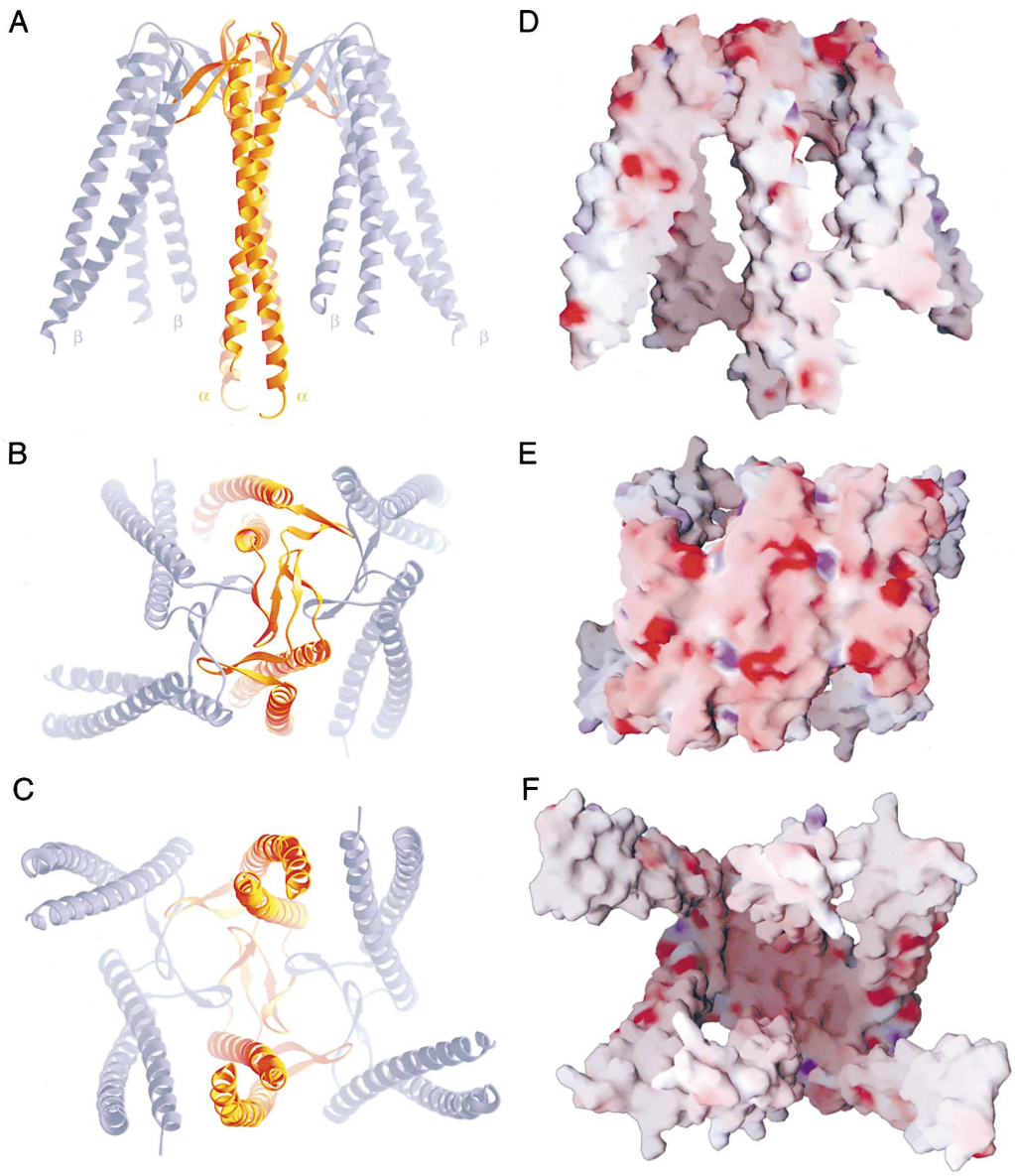

Figure 1. Structure of the Prefoldin Hexamer

(A-C) Ribbon representation of the prefoldin hexamer shown in different orientations (front, top, and bottom view). α class subunits are orange and β class subunits are silver. All ribbon diagrams were generated using Ribbons (Carson, 1997).

(D-F) The molecular surface of the prefoldin hexamer. The electrostatic potential is rendered onto the molecular surface of the hexamer that is shown in approximately the same orientations as in (A-C). Red color indicates acidic and blue basic surface regions. All surfaces were generated using GRASP (Nicholls et al., 1993).

ing mechanism of prefoldin. The yeast and bovine complexes, originally termed GimC (Genes involved in microtubule biogenesis Complex) and prefoldin, respectively, are each assembled from six different proteins (Geissler et al., 1998; Vainberg et al., 1998; Siegers et al., 1999). The archaeal counterpart from *Methanobacterium thermoautotrophicum* is a hexamer built from only two subunit types (Leroux et al., 1999). No sequence similarity exists between GimC/prefoldin and proteins with known structures, indicating that it belongs to a new class of molecular chaperones that possesses a novel structure and functional mechanism. Because of the high degree of evolutionary conservation of GimC/prefoldin complexes, the archaeal homologue will hereafter be referred to as prefoldin. Prefoldin (PFD) subunits can be subdivided into two classes, namely α and β. Archaea possess one member of each class (PFDα and PFDβ), and eukaryotes have two different but related subunits of the α class and four related subunits of the β class (Leroux et al., 1999). The archaeal complex is rich in α-helical structures, consistent with the prediction that prefoldin contains extensive coiled coil regions (Geissler et al., 1998, Leroux et al., 1999).

Several recent studies have provided insights into the role of prefoldin in protein biogenesis. Disruption of yeast genes encoding prefoldin subunits results in actin

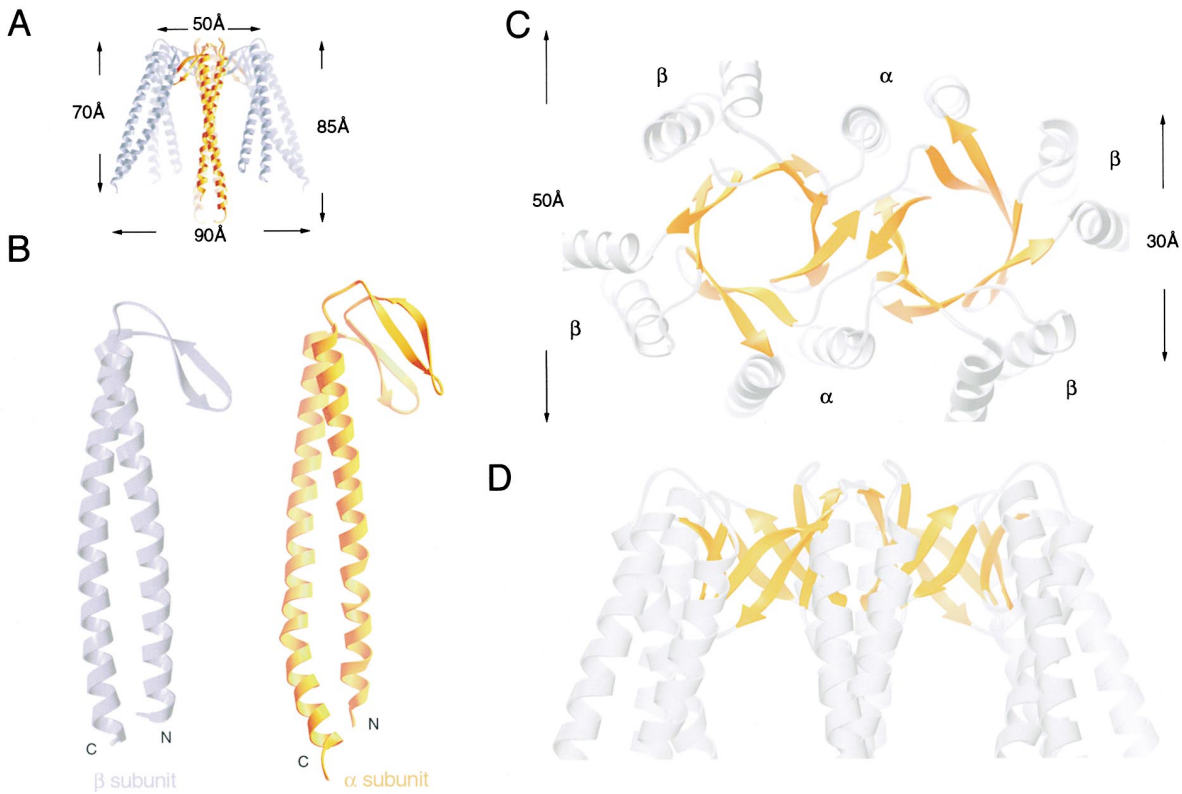

Figure 2. Details of the Prefoldin Architecture

(A) Approximate dimensions of the hexamer.

(B) Architecture of Prefoldin α and β class subunits.

(C and D): Details of the β barrel platform showing top and front views, respectively.

and tubulin cytoskeletal defects comparable to those of various yeast strains with temperature-sensitive defects in the chaperonin TRiC (Geissler et al., 1998; Vainberg et al., 1998; Siegers et al., 1999). Prefoldin binds nascent (or nonnative) chains of actins and tubulins and can transfer them to TRiC for folding (Vainberg et al., 1998; Hansen et al., 1999). Yeast and mammalian prefoldin have been suggested to interact directly with TRiC (Vainberg et al., 1998; Siegers et al., 1999), and yeast prefoldin has been shown to function as a cofactor of TRiC in accelerating the release of folded actin by the chaperonin in vivo (Siegers et al., 1999). Eukaryotic prefoldin might be specific for actins and tubulins (Hansen et al., 1999), but archaeal prefoldin binds numerous unrelated proteins of various sizes, a property that could reflect a more general role in protein folding (Leroux et al., 1999).

To provide a basis for understanding the structure and function of prefoldin complexes, we solved the crystal structure of the prefoldin hexamer from *M. thermoautotrophicum* and defined regions necessary for binding nonnative polypeptides.

Results and Discussion

Structure Determination

The 87 kDa archaeal prefoldin hexamer from the thermophile *M. thermoautotrophicum* (MtPFD) was assembled from purified subunits, as previously described (Leroux et al., 1999 and Experimental Procedures). Because crystals prepared from this complex diffracted only to moderate resolution, we defined a protease-resistant core containing the entire complex except for the last eight or nine residues of the MtPFDβ subunit. A truncated MtPFDβ protein lacking the last seven residues was produced and combined with wild-type MtPFDα to assemble a complex whose apparent subunit composition, size by gel filtration, far-UV spectrum, and chaperone activity is indistinguishable from that of the wild-type MtPFD complex (see Figures 6 and 7, as well as Leroux et al., 1999). We refer to this complex as Pα/Pβ, but for simplicity, describe the structure as that of prefoldin. The crystal structure of the prefoldin (Pα/Pβ) complex was solved and refined to 2.3 Å resolution as described under Experimental Procedures. The biologically active $\alpha_2\beta_4$ hexamer (Leroux et al., 1999) was derived unambiguously by applying crystal symmetry.

Overall Architecture of the Prefoldin Hexamer

The prefoldin hexamer complex has a unique quaternary structure resembling the shape of a jellyfish (Figure 1). A large central cavity is bordered by six long tentacles formed by rods of α-helical coiled coils. Individual coiled coil rods have lengths between 60 and 70 Å (Figure 2A and 2B). The coiled coil tentacles point away from a platform consisting of two eight-stranded up and down

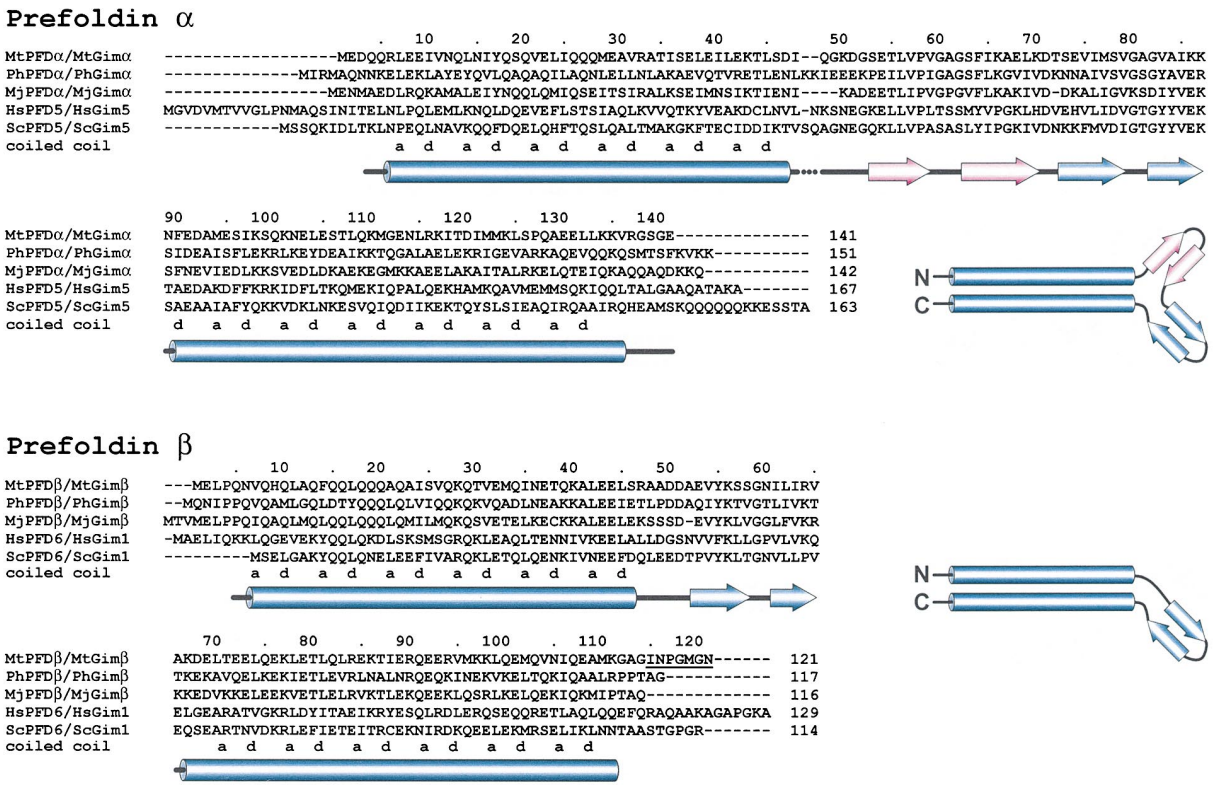

Figure 3. Alignment of α and β Class Subunits from Archaea and Eukaryotes

Sequence alignment of archaeal prefoldin subunits (Mt, *Methanobacterium thermoautotrophicum*; Ph, *Pyrococcus horikoshii*; Mj, *Methanococcus jannaschii*) with their closest *Saccharomyces cerevisiae* (Sc) and *Homo sapiens* (Hs homologs). Secondary structure elements are represented as cylinders (α helices) and arrows (β strands). The region of the extra β hairpin, present in the class subunit, is indicated by red arrows. Positions a and d of the heptad repeats making interhelix coiled coil contacts are labeled accordingly. The last seven residues of MtPFDβ (underlined) are missing in the crystallized form of the complex. To indicate the arrangement of secondary structure elements, schematic representations are shown for both classes of subunits.

β barrels with the approximate dimension of 15x30x50 Å^3 (Figure 2C and D). Each prefoldin subunit forms one coiled coil that is tightly anchored to the platform via its proximal end. There are virtually no interactions between the coiled coils from different subunits, and individual coiled coil rods are fully solvated and expose mostly charged and polar side chains to the solvent. In the crystal structure, the access to the cavity is not blocked by any structured elements. Because of its unusual architecture, the complex has a very large exposed surface area of about 35,000 Å^2, which is 1.75 times greater than the predicted average molecular surface area for an oligomeric protein of the same size (20,000 Å^2, calculated with a probe radius of 1.4 Å; Miller et al., 1987). The complex therefore has a rather limited hydrophobic core that is most pronounced in the region of the platform. The structure does not provide any evidence for the presence of a nucleotide binding site, in accordance with the apparent lack of an ATP-regulated protein function for both archaeal and eukaryotic prefoldin (Vainberg et al., 1998; Leroux et al., 1999).

Structures of the α and β Prefoldin Subunits

Based on the analysis of multiple sequence alignments, prefoldin/GimC subunits could be grouped into two evolutionary-related classes of sequences: α and β (Leroux et al., 1999). Consistent with secondary structure predictions (Leroux et al., 1999), the N- and C-terminal regions of the β class subunits form α helices that are connected by a β hairpin linker consisting of two short β strands (Figure 2B). The α helices arrange intramolecularly to form a two stranded antiparallel α-helical coiled coil. Prefoldin subunits of the α class have the same basic architecture, but the connecting linker consists of two β hairpins rather than one. The extra β hairpin is used for the dimerization of α subunit monomers (Figure 2C). These α dimers provide the core required for the formation of the hexamer (see below). A sequence alignment (Figure 3) shows PFDα and PFDβ subunits from three archaeal species, as well as PFD6 (Gim5) and PFD5 (Gim1) subunits from yeast and humans, which are representatives of the α and β classes of subunits, respectively. The high level of sequence and predicted secondary structure conservation between archaeal and all eukaryotic prefoldin α and β class subunits (Leroux et al., 1999) strongly suggest that the overall shape of prefoldin hexamers is highly conserved. Thus, the structure of the hexamer presented here provides a framework for understanding eukaryotic and archaeal prefoldin complexes in general.

The coiled coils formed by the α and β prefoldin subunits are structured regularly throughout most of the

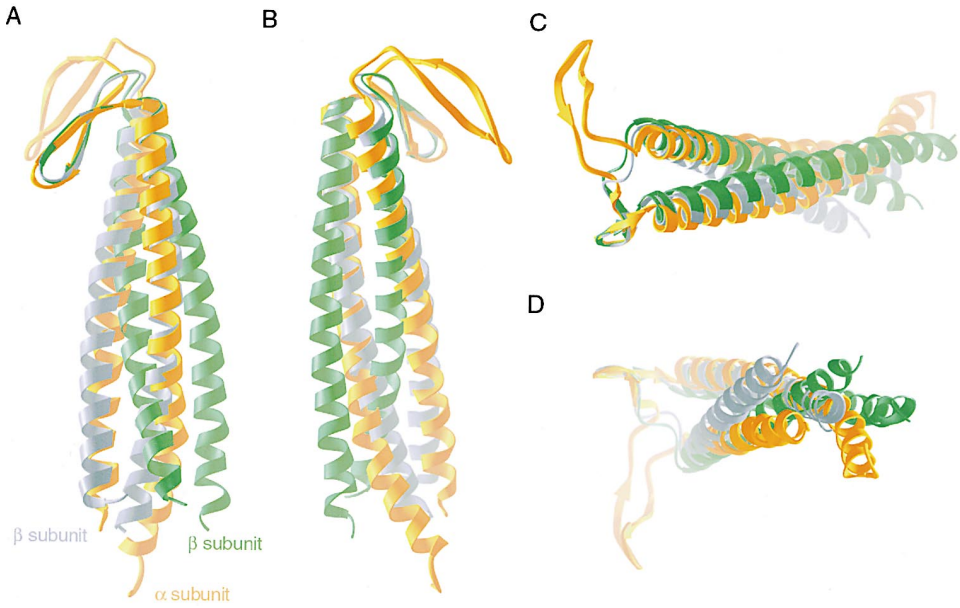

Figure 4. Mobility of the Coiled Coils

The three independent prefoldin subunits in the asymmetric unit were structurally aligned by superpositioning the conserved β hairpin. β subunits are colored silver and green, respectively, and the α subunit is shown in orange.

(A and B) Two different orthogonal views along the vertical axis of the coiled coils.

(C) View from the top of the platform.

(D) View from the distal ends of the coiled coils.

rods. In ideal two-stranded coiled coils, the heptad motif a-b-c-d-e-f-g is repeated n times and the a and d residues make up the hydrophobic core of the two-helix bundles (Crick, 1953; Lupas, 1996). This arrangement results in a knobs-into-holes packing of the hydrophobic core of the coiled coils, in which a hydrophobic residue of one α helix packs into a cavity formed by four hydrophobic residues of its partner helix.

The coiled coils of the two PFDβ subunits in the asymmetric unit are each about 40 residues long, resulting in 12 turns of both α helices. The C-terminal seven amino acids that were removed from this subunit in the Pα/Pβ complex would extend beyond the coiled coils. Interestingly, the sequence of the PFDβ subunit from Methanococcus jannaschii ends precisely where MtPFDβ was truncated (Figure 3), suggesting that these residues are not critical for biological activity. The two α helices of the PFDα subunit are 11 and 13 turns in length, respectively. Here, the longer C-terminal α helix deviates from ideality toward the distal tip of the coiled coil (Figure 2B). This distortion is most likely the result of packing interactions in the crystal as the very C-terminal residues of the α subunit make contacts with the top surface of the platform of a crystallographically related trimer (not shown). As a consequence, the C-terminal α helix of the α subunit is kinked at residue Met_{122}.

Near the distal end of the rods, the coiled coils of both the α and β subunits become partially untwisted, leading to the exposure of parts of the hydrophobic interface. This exposure of a and d residues of the heptad repeats creates hydrophobic patches near the ends of the coiled coils. The possible functional significance of these hydrophobic patches will be discussed in more detail below.

Assembly of the Prefoldin Hexamer

The prefoldin hexamer is assembled from the central regions of all six subunits. These regions form two β hairpins in the α class and one β hairpin in the β class subunits. The four β hairpins of the two α class subunits provide the central core for the assembly of two 8 stranded up and down β barrels (Figure 2C and 2D). Dimerization of the PFDα monomers is achieved by the extra hairpin (residues 53 to 70) and each α subunit participates in the formation of both β barrels. In isolation, PFDα subunits readily form dimers that are stable in solution. They provide the structural nucleus for hexamer formation upon addition of four PFDβ subunits that are most likely monomeric in the absence of PFDα (Leroux et al., 1999). The β barrels have a densely packed hydrophobic core with predominantly large hydrophobic amino acid side chains from the β strand regions pointing into the center. The cylinders formed by the β barrels are completely filled by hydrophobic side chains and do not form pores.

Flexibility of the Coiled Coils

From the spatial arrangement of the three different coiled coil rods in the asymmetric unit (Figure 4), it is apparent that the prefoldin complex is not a rigid entity. Individual tentacles seem to have considerable flexibility and come off the β barrel platform at different angles. It is likely that their orientation, as observed in the crystal, is influenced by crystal packing, and that individual coiled coils will be rather flexible in solution, especially at the growth temperature of the host organism (65°C). Such conformational flexibility may be functionally relevant for the interaction with a wide range of nonnative substrates.

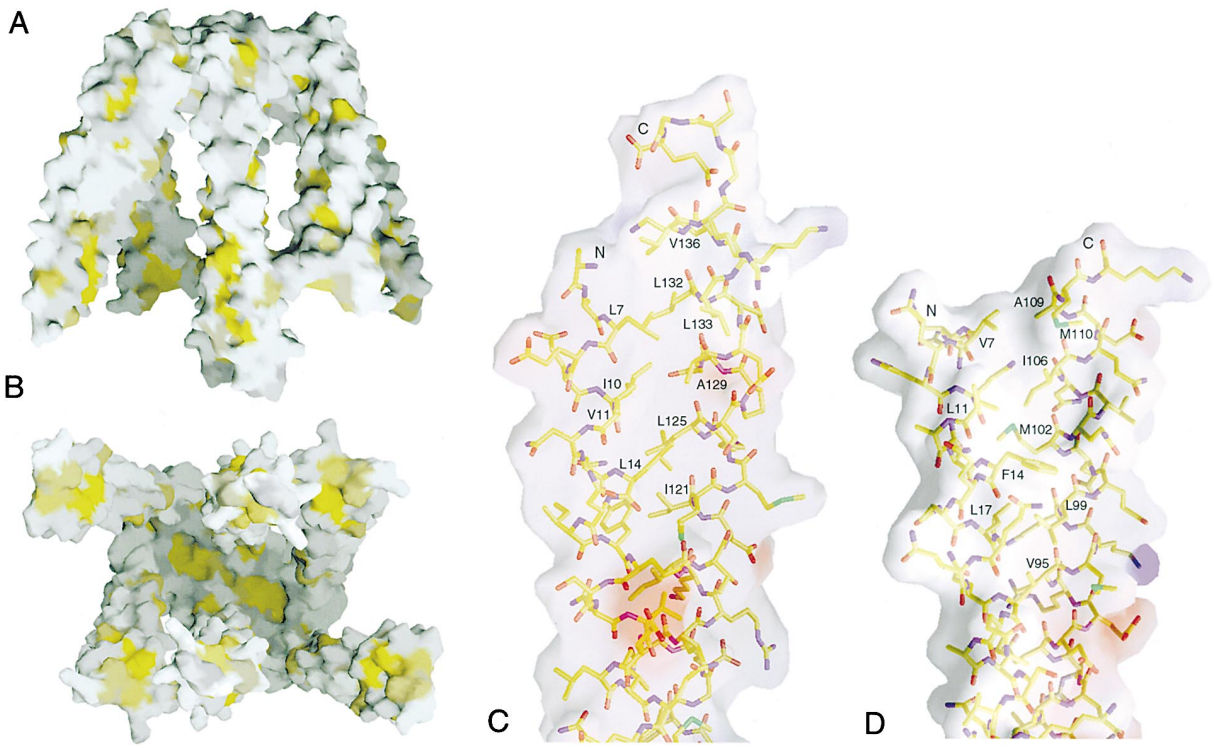

Figure 5. Hydrophobic Patches on the Molecular Surface of Prefoldin

(A and B) The hydrophobicity of the 20 amino acid side chains (Roseman, 1988) was mapped onto the molecular surface of the hexamer using GRASP. The most hydrophobic regions are colored in yellow and hydrophilic regions are gray.

(C and D) Details of the proximal regions of the α and β subunit tentacles. Partially solvent exposed residues of the hydrophobic coiled coil interface are labeled.

Eukaryotic Prefoldin Structure

The archaeal structure described here is the most basic version of a prefoldin hexamer, with only one type of α and one type of β class subunit forming the hexamer. In eukaryotes, six different genes encode prefoldin subunits, and prefoldin hexamers are assembled from all six subunits (Vainberg et al., 1998; Siegers et al., 1999). The two eukaryotic α class subunits (PFD3/Gim2 and PFD5/Gim5) most likely form the α dimer core, and the four different β subunits (PFD6/Gim1, PFD4/Gim3, PFD2/Gim4, and PFD1/Gim6) complete the hexamer (Leroux et al., 1999). The more complex subunit composition of eukaryotic prefoldin may be required for its apparently more specialized role in recognizing actins and tubulins (Hansen et al., 1999; Leroux and Hartl, 2000). Substrate specificity could be determined by local sequence variations in individual subunits, resulting in unique surface properties for the different coiled coils.

Deletion of the Coiled Coil Tips Impairs Prefoldin Activity

The quaternary structure of prefoldin does not bear any resemblance to other known molecular chaperone structures (Saibil, 2000). Although eukaryotic prefoldin cooperates functionally with the cytosolic chaperonin, it is obvious from the structural data presented here that it is not an analog of the bacterial group I chaperonin cofactor. The all β sheet GroES heptamer serves as a lid that covers the cavity of GroEL and couples the GroEL ATPase cycle to protein folding, but does not itself interact with unfolded proteins (Sigler et al., 1998).

This lack of structural homology to known chaperones raises the question of how prefoldin functions in preventing the aggregation of nascent and unfolded proteins, and how it might interact and cooperate with the group II chaperonin. Most of the accessible molecular surface of prefoldin is hydrophilic (Figure 1 D-F) and displays a large number of charged and polar side chains such as glutamic acid and glutamine residues, which are unlikely to interact with hydrophobic peptide sequences. Regions where hydrophobic residues are surface-exposed are the accessible parts of the hydrophobic core of the β barrels at the bottom of the cavity and the distal end regions of the coiled coil tentacles (Figure 1 D-F and Figure 5). Being readily accessible, the distal regions of the tentacles are likely candidates for the initial interaction with substrate molecules. Here, due to local untwisting of the coiled coils, parts of the residues that form the hydrophobic interface between neighboring helices (a and d residues of the heptad repeat) are accessible to solvent, resulting in the display of hydrophobic surface patches that might be used for interaction with substrates (Figure 5C and D).

To investigate the involvement of the distal regions of the coiled coils in stabilizing unfolded proteins, we assembled complexes with truncation mutants of PFDα

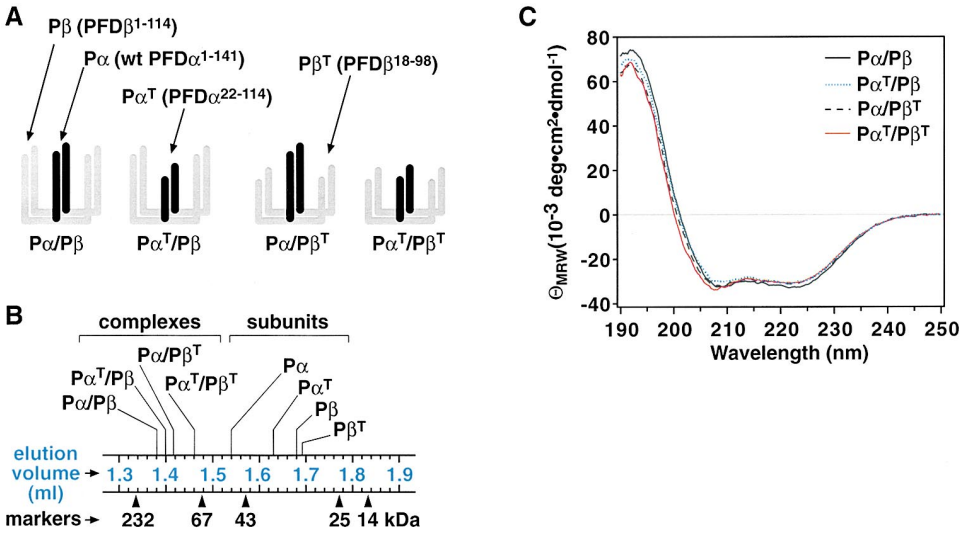

Figure 6. Structural Characterization of Truncated Prefoldin Hexamers

(A) Schematic representations of prefoldin complexes assembled from wild-type and/or truncated prefoldin subunits. MtPFDα subunits (α) are shown in black and MtPFDβ (β) subunits in gray. The amino acids present in the truncation mutants ("T") are shown, and the names of complexes built from wild-type and/or mutants are indicated below each structure.

(B) Elution of wild-type and truncated prefoldin subunits and complexes from a Superdex 200 size exclusion column. The peak elution volumes of the protein species (top) are shown compared to molecular weight markers (bottom; see Experimental Procedures).

(C) Circular dichroism spectra of the truncated prefoldin complexes (1–2 μM) in 20 mM $NaPO_4$ pH 8.0 buffer at 20°C. Data shown are averages of four scans.

and PFDβ subunits. In these mutants, the distal parts of the coiled coils were shortened by three α-helical turns in the PFDβ subunit and by five α-helical turns in the longer PFDα subunit, resulting in the removal of the distal hydrophobic patches. Three different complexes were assembled: one lacking the two ends of the α subunits ($P\alpha^T/P\beta$; T signifies "truncated"), one lacking the four ends of the four β subunits ($P\alpha/P\beta^T$), and another lacking the ends of all six α and β tentacles ($P\alpha^T/P\beta^T$) (Figure 6A). The assembled complexes and individual subunits eluted from an analytical size exclusion column in the order expected based on their structures and molecular weights (Figure 6B). We also verified that the overall conformation of the mutant complexes was unchanged relative to the Pα/Pβ prefoldin hexamer. Far-UV circular dichroism measurements showed that the truncated mutant complexes possess spectra very similar to wild-type archaeal prefoldin (Figure 6C and Leroux et al., 1999). In addition, the melting temperatures of the truncated complexes ($T_m \geq 60°C$) were comparable to that of Pα/Pβ (70°C) (not shown). These data demonstrate that the truncated prefoldin complexes assume correctly assembled, stable conformations in solution.

M. thermoautotrophicum prefoldin is capable of stabilizing a number of nonnative proteins, preventing them from aggregating upon dilution from denaturant into buffer as monitored spectrophotometrically at 320 nm (Leroux et al., 1999). We determined the ability of the various complexes with truncated coiled coils to affect the aggregation behavior of chemically denatured bovine mitochondrial rhodanese (33 kDa). Whereas Pα/Pβ almost completely prevented the aggregation of denatured rhodanese at a ratio approaching 1 prefoldin hexamer to 1 rhodanese molecule (Figure 7A), $P\alpha/P\beta^T$ and $P\alpha^T/P\beta^T$ complexes were ineffective in preventing aggregation even at a 9-fold molar excess of the complexes over the substrate (Figure 7B). Removing the distal coiled coil regions of the two PFDα subunits in the hexamer resulted in a $P\alpha^T/P\beta$ complex that had a strongly impaired, but still detectable, activity in preventing rhodanese aggregation in vitro. At a 3-fold molar excess over rhodanese, $P\alpha^T/P\beta$ was barely active, but at a 9-fold (or higher) molar excess, it slowed rhodanese aggregation considerably (Figure 7B).

Similar observations were made with the 62 kDa protein firefly luciferase as the substrate. Radiolabeled, native luciferase produced by in vitro translation in reticulocyte lysate (Figure 7C, lane 1) was mixed with buffer, 2 μM Pα/Pβ or 4 μM $P\alpha^T/P\beta$ and incubated at 42°C for 5 min to allow for unfolding of the thermally labile luciferase (Schröder et al., 1993). Binding reactions were then separated on a native polyacrylamide gel. Compared with the buffer control, incubation of luciferase with Pα/Pβ gave a distinct radiolabel-containing band that comigrated exactly with the Pα/Pβ complex (indicated by a black arrowhead; Figure 7C, compare lanes 2 and 3). Excision of this band and subsequent analysis by SDS-PAGE revealed mostly full-length luciferase (Figure 7C, lanes 3 and 5). In contrast, no interaction between prefoldin and luciferase was observed upon incubation with twice the amount of $P\alpha^T/P\beta$ (Figure 7C, lane 4), even though the mutant chaperone complex is stable at 42°C (as reported above) and migrates on the native gel in essentially the same position as Pα/Pβ.

Together, these data indicate that the distal regions of the coiled coils from both prefoldin subunits (α and β) are required for full chaperone activity of the complex.

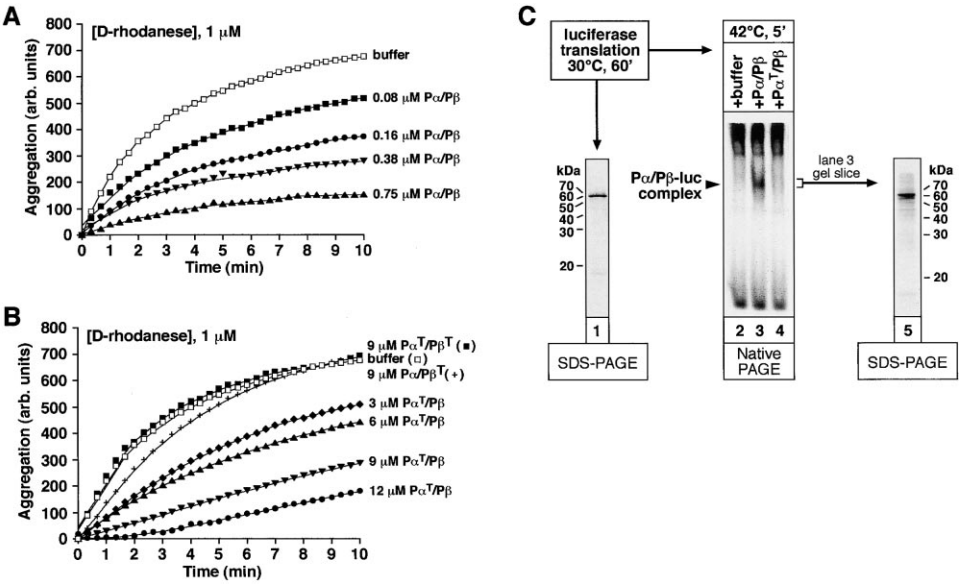

Figure 7. Efficient Interaction of Prefoldin with Unfolded Rhodanese (33 kDa) and Firefly Luciferase (62 kDa) Requires the Ends of All Six Coiled Coils

(A) Inhibition of aggregation of denatured rhodanese (1 μM) by increasing amounts of Pα/Pβ complex. Guanidine-denatured rhodanese (100 μM) was diluted 100-fold into a solution containing buffer or various concentrations of Pα/Pβ complex (concentrations as indicated on the right). Rhodanese aggregation at 25°C was monitored at 320 nm for 10 min.

(B) Effect of prefoldin truncation mutants on the aggregation of rhodanese. Denatured rhodanese was diluted as above into solutions containing buffer only or various amounts of $P\alpha^T/P\beta$, $P\alpha/P\beta^T$ or $P\alpha^T/P\beta^T$ (as indicated on the right), and rhodanese aggregation was measured as in (A).

(C) Pα/Pβ forms a detectable binary complex with nonnative firefly luciferase, whereas the $P\alpha^T/P\beta$ truncated mutant does not. Native firefly luciferase was prepared in a rabbit reticulocyte coupled transcription/translation system. Aliquots of the translation were analyzed directly by SDS-PAGE (lane 1) or incubated with buffer (lane 2), 2 μM Pα/Pβ (lane 3) or 4 μM $P\alpha^T/P\beta$ complexes (lane 4). Reactions 2–4 were incubated for 5 min at 42°C to allow complex formation with the thermolabile firefly luciferase, and analyzed on a nondenaturing gel. The position of Pα/Pβ, $P\alpha^T/P\beta$ and Pα/Pβ-luciferase complexes on the native gel is shown by a black arrowhead. The identity of the radiolabeled species comigrating with Pα/Pβ was confirmed by excising the band in lane 3 and reanalyzing it by SDS-PAGE (lane 5).

Substrate binding to prefoldin appears to be multivalent, requiring both classes of subunits at the same time. Notably, the contribution of the four PFDβ subunits present in the complex is apparently greater than the contribution of the PFDα dimer. Eukaryotic prefoldin only binds stably to nascent actin chains if they are at least roughly 145 residues in length, and stable cotranslational interaction with tubulin chains can only be observed when about 250 residues have been synthesized (Hansen et al., 1999). These observations are consistent with the synergistic action of multiple weak binding sites for unfolded proteins on prefoldin. Our results also explain why isolated archaeal prefoldin subunits are inactive in preventing the aggregation of nonnative proteins (Leroux et al., 1999).

A contribution to substrate binding by the hydrophobic surfaces that are deep inside the cavity cannot be ruled out. Here, parts of the side chains that build the hydrophobic core of the β barrels are exposed to solvent (Figure 5B). These regions might also interact with hydrophobic surfaces of client proteins. It is clear from the above deletion experiments however, that these surface regions of prefoldin are not sufficient to maintain chaperone function in the absence of the end regions of the coiled coils where the hydrophobic patches are present in the crystal structure. Nevertheless, it is conceivable that the cavity formed by the six protruding coiled coils acts as a pocket that could (partially) envelop a substrate.

A Novel Class of Molecular Chaperone

Prefoldin has a unique quaternary structure that has no counterpart in other known molecular chaperones or protein complexes in general. We note, however, that prefoldin exhibits a remote but interesting similarity to the TolC trimer, an integral membrane pore complex (Koronakis et al., 2000). In TolC, the transmembrane pore is formed by β hairpins arranged into a single 12-stranded β barrel platform and six long α helical coiled coils that pack against each other to form a channel that extends from the platform. The distal ends of the coiled coils are untwisted and implicated in the interaction with translocases.

From the structural and functional data presented here, a speculative model of how prefoldin functions at the molecular level can be proposed. The finding that prefoldin from a thermophilic organism is active as a chaperone at ambient temperatures (Figure 7 and Leroux et al., 1999) suggests that the prevention of aggregation of nonnative proteins is in large part dominated by surface-surface interactions. Indeed, hydrophobic patches are displayed by the distal regions of the coiled coils and point mostly toward the central cavity in all six prefoldin subunits in the crystal (Figure 1C-E and Figure 5). The regions encompassing the hydrophobic patches are required for the multivalent interaction with unfolded or partially folded proteins.

On the other hand, the observation that the prefoldin tentacles appear to have considerable flexibility (Figure

Table 1. Data Collection, Phasing and Refinement Statistics

Data Collection[a]				
Space group		$P2_12_12$		
Unit cell (Å^3)		a = 72.85 b = 90.69 c = 78.68		
	E1	E2	E3	E4
X-ray source		DESY, BW6[b]		
Wavelength (Å)	λ = 0.9794	λ = 0.9802	λ = 0.9500	λ = 1.0510
Resolution (Å)		30.0–2.3 (2.38–2.30)		30–2.45 (2.54–2.45)
I/σ_I	24.4 (6.0)	24.5 (6.5)	23.4 (6.0)	26.8 (6.5)
Completeness (%)	99.7 (99.5)	99.7 (99.6)	99.6 (99.6)	99.6 (97.5)
R_{sym} (%)	4.3 (18.5)	4.4 (18.8)	4.4 (19.6)	4.1 (15.9)
MAD Phasing[c]				
Anomalous scatterer		10 Se		
Resolution (Å)		30.0–2.7		
Figure of merit		0.463		
R_{cullis_ano}	0.73	0.96	0.79	0.98
Phasing power centric	0.14	–	0.65	0.58
Phasing power acentric	0.17	–	0.81	0.80
Refinement Statistics[d]				
Resolution (Å)		20–2.3		
# reflections R_{work}/R_{free}		21593/1976		
R_{work}/R_{free} (%)[e]		21.8/26.6		
# of protein atoms		2756		
# solvent molecules		333		
R.m.s.d. bond length (Å)		0.008		
R.m.s.d. angles (°)		1.2		

[a] Values as defined in SCALEPACK (Otwinowski and Minor, 1997), Bijvoet pairs separated.
[b] Deutsches Elektronen Synchrotron in Hamburg, beamline BW6.
[c] Unweighted values as defined in MLPHARE (CCP4, 1994).
[d] Values as defined in CNS (Bruenger et al., 1998).
[e] No sigma cutoffs.

4) suggests that, in solution, the hexamer is capable of adjusting to the different spatial requirements of individual substrate molecules, including nascent chains and partially folded proteins. The multivalent binding of the otherwise very hydrophilic prefoldin complex to substrates results in a detergent-like solubilization of polypeptides prone to aggregation in their nonnative states. It seems possible that bound substrates protrude into the central cavity formed by the coiled coil tentacles, resulting in the shielding of aggregation-prone states from the bulk solution. Because exposure of the hydrophobic patches is a result of the partial untwisting of the coiled coils, it is conceivable that upon binding hydrophobic regions of substrate proteins, further unwinding of the coiled coils may occur, thus exposing more hydrophobic regions in the chaperone.

Unlike Hsp70 or chaperonins, prefoldin does not regulate substrate binding and release by ATP binding and hydrolysis (Vainberg et al., 1998; Leroux et al., 1999). The use of multiple weak interaction sites for substrate binding may therefore provide a simple means of making the binding of nonnative polypeptide substrates reversible for downstream completion of folding. While the combination of at least six binding sites results in a sufficiently strong interaction with substrate proteins, binding to individual tentacles may be relatively weak and reversible. As a result, substrates may be passed to other chaperones that bind with higher affinity and mediate completion of the folding reaction, most likely a chaperonin.

In the case of the eukaryotic, and perhaps the archaeal prefoldin-chaperonin system, specific interactions between the two chaperones may help to provide a sequestered environment in which nonnative polypeptides fold efficiently, without undergoing off-pathway events that would lead to misfolding and aggregation (Vainberg et al., 1998; Siegers et al., 1999). Based on the archaeal prefoldin structure, one may speculate that the distal regions of one or more of the prefoldin subunits might interact with specific sites on the chaperonin (e.g., the apical domains), effectively juxtapositioning the two substrate binding sites of the chaperones, and therefore facilitating substrate transfer from one to the other. It remains to be established whether such a direct interaction occurs.

Experimental Procedures

Production of Wild-Type and Mutant Prefoldin Complexes

Wild-type and truncated versions of *M. thermoautotrophicum* α and β prefoldin subunits were generated by PCR amplification of the full-length genes and cloned into the bacterial expression vector pRSET6a at the *Nde*I/*Bam*HI site (Leroux et al., 1999). The abbreviated names and sequences of the prefoldin proteins used are as follows: Pα, wild-type MtPFD (residues 1–141); $P\alpha^T$, encompasses residues 22–114 of wild-type MtPFD; Pβ, residues 1–114 of wild-type MtPFDβ; $P\beta^T$, residues 18–98 of wild-type MtPFDβ. Both $P\alpha^T$ and $P\beta^T$ contain an additional methionine (start codon) at their N terminus. Proteins were expressed in *E. coli* and were purified as described previously (Leroux et al., 1999), except for $P\alpha^T$ and $P\beta^T$, which were purified by successive chromatography on Q-sepharose and S-100HR columns (Pharmacia). Complexes were assembled by

diluting α and β subunits (at a ratio of 1 to 2.2) into 4M urea/20 mM Tris pH 8.0 buffer, followed by equilibrium dialysis in LS buffer (20 mM $NaPO_4$ pH 8.0). The complexes were further purified by separation on an S-200HR sizing column in LS buffer. The constructs were sequenced, and protein identities were confirmed by mass spectrometry.

Crystallization and Crystal Handling

The purified and assembled full-length prefoldin hexamer readily crystallized under a variety of conditions. To improve the diffraction properties of the crystals, limited proteolysis was performed with the aim of identifying unstructured regions. The C-terminal eight or nine residues of the β subunit were removed by proteinase K or subtilisin, as determined by mass spectrometry and sequencing. A truncated PFDβ protein lacking the last seven residues was produced and combined with wild-type PFDα subunit to generate a complex we refer to as Pα/Pβ (Figure 6A). The best crystals were obtained in a hanging drop setup by mixing equal volumes of prefoldin hexamer (protein concentration of 10 mg/ml) and reservoir buffer (800 mM sodium acetate and 20% ethylene glycol) at 21°C. After one week of incubation at 21°C, the temperature was shifted to 4°C, where crystals appeared readily after one week. Crystals belonged to the space group P21212 with a $\alpha_1\beta_2$ trimer in the asymmetric unit. Crystals of the truncated complex diffracted significantly better, and a data set could be collected at the temperature of 100 k to a resolution limit of 2.7 Å (our unpublished data). For phasing, the Pβ subunit was labeled with selenomethionine (SeMet) (Scheufler et al., 2000), and the complex reconstituted using unlabeled PFDα subunit. The SeMet-derivatized complexes crystallized under identical conditions as the wild-type protein but diffracted to at least 2.2 Å resolution.

The incorporation of six SeMet residues per β subunit was verified by mass spectrometry. The selenomethionyl $\alpha_2\beta_4$ hexamer (containing a total of 24 selenium atoms) was as active as wild-type MtPFD in chaperone assays (not shown). A comparison of the wild-type and the SeMet-containing structures revealed no differences in the tracing of the protein backbones. Because the crystals of the SeMet-labeled complex diffracted to much higher resolution, only this structure is presented herein.

Data Collection and Structure Determination

A four-wavelength MAD experiment was performed using data collected from a single cryo-cooled crystal at the Max-Planck beamline BW6 (DESY Hamburg). Data was collected using a MAR CCD detector (MAR Research Hamburg) and processed using DENZO and Scalepack (Otwinowski and Minor, 1997). By treating MAD as a special case of MIR, the program SOLVE (Terwilliger and Berendzen, 1999) readily identified 10 of the 12 selenium sites. After phasing with MLPHARE and solvent correction by DM (CCP4, 1994), a partial model was automatically built into the resulting electron density using the program wARP (Perrakis et al., 1999). This partial model consisted of the entire β barrel platform and most of the two PFDβ subunits present in the asymmetric unit. The remaining parts of the final model were fitted manually into electron density during iterative cycles of model building using O (Jones et al., 1991) and torsion angle refinement of the models as implemented in CNS (Brunger et al., 1998). Detailed statistics of the data collection phasing and refinement steps are summarized in Table 1. Owing to disorder, some N and C-terminal residues in all three chains are missing from the final model. In the α subunit (chain C), residues 5–141 were built and in the two β subunits residues 5–111 (chain A) and 6–111 (chain B), respectively, are included in the final model.

Size Exclusion Chromatography (SEC)

All combinations of prefoldin complexes made with wild-type and/or truncated subunits assembled as efficiently as wild-type MtPFD. The relative elution volume of the different prefoldin complexes, individual subunits, and molecular weight markers was determined from analytical SEC on a Superdex 200 PC3.2/30 column (Pharmacia) in 20 mM Tris pH 8.0/100 mM NaCl at room temperature. The molecular weight standards used were: catalase (232 kDa), bovine serum albumin (67 kDa), ovalbumin (43 kDa), chymotrypsinogen A (29 kDa), and ribonuclease A (14kDa).

Prevention of Rhodanese Aggregation Assays

The effect of various concentrations of MtPFD complexes on the aggregation of denatured rhodanese diluted 100-fold from guanidine-HCl (final concentration 1 μM) into LS buffer was monitored spectrophotometrically over a period of 10 min by following the change in turbidity of the solutions at 320 nm and 25°C. Denatured rhodanese was prepared in 6 M guanidine hydrochloride, 20 mM Tris pH 8.0, 100 mM NaCl, and 1 mM $MgCl_2$ (Leroux et al., 1999).

Complex Formation with Firefly Luciferase

Native, [^{35}S]-methionine-labeled firefly luciferase was prepared by coupled transcription/translation in a reticulocyte lysate system (Promega) (Frydman et al., 1994) using the supplied pGEM-luc vector. Following 1 hr translations at 30°C, aliquots were combined with either LS buffer, 2 μM Pα/Pβ, or 4 μM $P\alpha^T$/Pβ complexes and incubated for 5 min at 42°C to allow binary complex formation (note that luciferase denatures rapidly at this temperature; Schröder et al., 1993). Reactions were then separated on 4.5% native polyacrylamide gels made and run in 80 mM MOPS-KOH pH 7.0, followed by autoradiography. To verify the identity of the radiolabeled protein bound to Pα/Pβ, bands corresponding to the position of the complex were excised and analyzed by 16% SDS-PAGE.

Circular Dichroism Measurements

Far-UV circular dichroism spectra of prefoldin complexes (1–2 μM in LS buffer) were recorded from 250 to 190 nm on a JASCO J-720 spectropolarimeter at 20°C (Leroux et al., 1999). Spectra shown are an average of four scans.

Miscellaneous

Protein concentrations were determined by UV measurements based on their predicted extinction coefficients at 276 nm. Molar concentrations given are for prefoldin hexamers and rhodanese monomers.

Acknowledgments

The authors thank Hans Bartunik and Gleb Bourenkov for help with data collection at the Max-Planck beamline BW6 (DESY Hamburg) and Marcus Fändrich for his help with the purification of wild-type prefoldin subunits and assembly of complexes. M. R. L. acknowledges support from an EMBO fellowship.

Received July 27, 2000; revised September 21, 2000.

References

Beckmann, R.P., Mizzen, L.E., and Welch, W.J. (1990). Interaction of Hsp70 with newly-synthesized proteins: implications for protein folding and assembly. Science *248*, 850–854.

Braig, K., Otwinowski, Z., Hegde, R., Boisvert, D.C., Joachimiak, A., Horwich, A.L., and Sigler, P.B. (1994). The crystal structure of the bacterial chaperonin GroEL at 2.8 Å. Nature *371*, 578–586.

Brunger, A.T., Adams, P.D., Clore, G.M., DeLano, W.L., Gros, P., Grosse-Kunstleve, R.W., Jiang, J.S., Kuszewski, J., Nilges, M., Pannu, N.S., et al. (1998). Crystallography & NMR system: A new software suite for macromolecular structure determination. Acta Crystallogr. D Biol. Crystallogr. *54*, 905–921.

Bukau, B., and Horwich, A.L. (1998). The Hsp70 and Hsp60 chaperone machines. Cell *92*, 351–366.

Carson, M. (1997). Ribbons. Methods Enzymol. *277*, 493–505.

CCP4 (Collaborative Computational Project Number 4). (1994). The CCP4 Suite – programs for protein crystallography. Acta Crystallogr. D *50*, 760–763.

Chen, L., and Sigler, P.B. (1999). The crystal structure of a GroEL/peptide complex: plasticity as a basis for substrate diversity. Cell *99*, 757–768.

Chen, S., Roseman, A.M., Hunter, A.S., Wood, S.P., Burston, S.G., Ranson, N.A., Clarke, A.R., and Saibil, H.R. (1994). Location of a folding protein and shape changes in GroEL-GroES complexes imaged by cryo-electron microscopy. Nature *371*, 261–264.

Coyle, J.E., Texter, F.L., Ashcroft, A.E., Masselos, D., Robinson, C.V., and Radford, S.E. (1999). GroEL accelerates the refolding of hen lysozyme without changing its folding mechanism. Nat. Struct. Biol. *6*, 683–690.

Crick, F.H.C. (1953). The packing of α-helices: simple coiled coils. Acta Crystallogr. *6*, 689–697.

Deuerling, E., Schulze-Specking, A., Tomoyasu, T., Mogk, A., and Bukau, B. (1999). Trigger factor and DnaK cooperate in folding of newly synthesized proteins. Nature *400*, 693–696.

Ditzel, L., Lowe, J., Stock, D., Stetter, K.O., Huber, H., Huber, R., and Steinbacher, S. (1998). Crystal structure of the thermosome, the archaeal chaperonin and homolog of CCT. Cell *93*, 125–138.

Eggers, D.K., Welch, W.J., and Hansen, W.J. (1997). Complexes between nascent polypeptides and their molecular chaperones in the cytosol of mammalian cells. Mol. Biol. Cell *8*, 1559–1573.

Ellis, R.J., and Hartl, F.U. (1999). Principles of protein folding in the cellular environment. Curr. Opin. Struct. Biol. *9*, 102–110.

Ewalt, K.L., Hendrick, J.P., Houry, W.A., and Hartl, F.U. (1997). In vivo observation of polypeptide flux through the bacterial chaperonin system. Cell *90*, 491–500.

Fenton, W.A., Kashi, Y., Furtak, K., and Horwich, A.L. (1994). Residues in chaperonin GroEL required for polypeptide binding and release. Nature *371*, 614–619.

Fink, A.L. (1999). Chaperone-mediated protein folding. Physiol. Rev. *79*, 425–449.

Frydman, J., Nimmesgern, E., Erdjument-Bromage, H., Wall, J.S., Tempst, P., and Hartl, F.U. (1992). Function in protein folding of TRiC, a cytosolic ring complex containing TCP-1 and structurally related subunits. Embo. J. *11*, 4767–4778.

Frydman, J., Nimmesgern, E., Ohtsuka, K., and Hartl, F.U. (1994). Folding of nascent polypeptide chains in a high molecular mass assembly with molecular chaperones. Nature *370*, 111–117.

Gao, Y., Thomas, J.O., Chow, R.L., Lee, G.H., and Cowan, N.J. (1992). A cytoplasmic chaperonin that catalyzes beta-actin folding. Cell *69*, 1043–1050.

Geissler, S., Siegers, K., and Schiebel, E. (1998). A novel protein complex promoting formation of functional alpha- and gamma-tubulin. Embo. J. *17*, 952–966.

Gribaldo, S., Lumia, V., Creti, R., de Macario, E.C., Sanangelantoni, A., and Cammarano, P. (1999). Discontinuous occurrence of the hsp70 (dnaK) gene among Archaea and sequence features of HSP70 suggest a novel outlook on phylogenies inferred from this protein. J. Bacteriol. *181*, 434–443.

Gutsche, I., Essen, L.O., and Baumeister, F. (1999). Group II chaperonins: New TRiC(k)s and turns of a protein folding machine. J. Mol. Biol. *293*, 295–312.

Hansen, W.J., Cowan, N.J., and Welch, W.J. (1999). Prefoldin-nascent chain complexes in the folding of cytoskeletal proteins. J. Cell Biol. *145*, 265–277.

Hartl, F.U. (1996). Molecular chaperones in cellular protein folding. Nature *381*, 571–579.

Hlodan, R., Tempst, P., and Hartl, F.U. (1995). Binding of defined regions of a polypeptide to GroEL and its implications for chaperonin-mediated protein folding. Nat. Struct. Biol. *2*, 587–595.

Horwich, A.L., Low, K.B., Fenton, W.A., Hirshfield, I.N., and Furtak, K. (1993). Folding in vivo of bacterial cytoplasmic proteins: role of GroEL. Cell *74*, 909–917.

Houry, W.A., Frishman, D., Eckerskorn, C., Lottspeich, F., and Hartl, F.U. (1999). Identification of in vivo substrates of the chaperonin GroEL. Nature *402*, 147–154.

Jones, T.A., Zou, J.Y., Cowan, S.W., and Kjeldgaard, M. (1991). Improved methods for building protein models in electron-density maps and the location of errors in these models. Acta Crystallogr. Section A *47*, 110–119.

Kim, S., Willison, K.R., and Horwich, A.L. (1994). Cystosolic chaperonin subunits have a conserved ATPase domain but diverged polypeptide-binding domains. Trends Biochem. Sci. *19*, 543–548.

Klumpp, M., Baumeister, W., and Essen, L.O. (1997). Structure of the substrate binding domain of the thermosome, an archaeal group II chaperonin. Cell *91*, 263–270.

Kobayashi, N., Freund, S.M., Chatellier, J., Zahn, R., and Fersht, A.R. (1999). NMR analysis of the binding of a rhodanese peptide to a minichaperone in solution. J. Mol. Biol. *292*, 181–190.

Koronakis, V., Sharff, A., Koronakis, E., Luisi, B., and Hughes, C. (2000). Crystal structure of the bacterial membrane protein TolC central to multidrug efflux and protein export. Nature *405*, 914–919.

Kubota, H., Hynes, G., and Willison, K. (1995). The chaperonin containing t-complex polypeptide 1 (TCP-1). Multisubunit machinery assisting in protein folding and assembly in the eukaryotic cytosol. Eur. J. Biochem. *230*, 3–16.

Langer, T., Pfeifer, G., Martin, J., Baumeister, W., and Hartl, F.U. (1992). Chaperonin-mediated protein folding: GroES binds to one end of the GroEL cylinder, which accomodates the protein substrate within its central cavity. Embo. J. *11*, 4757–4765.

Leroux, M.R., Fändrich, M., Klunker, D., Siegers, K., Lupas, A.N., Brown, J.R., Schiebel, E., Dobson, C.M., and Hartl, F.U. (1999). MtGimC, a novel archaeal chaperone related to the eukaryotic chaperonin cofactor GimC/prefoldin. Embo. J. *18*, 6730–6743.

Leroux, M.R., and Hartl, F.U. (2000). Protein folding: versatility of the cytosolic chaperonin TRiC/CCT. Curr. Biol. *10*, R260–264.

Llorca, O., Smyth, M.G., Carrascosa, J.L., Willison, K.R., Radermacher, M., Steinbacher, S., and Valpuesta, J.M. (1999). 3D reconstruction of the ATP-bound form of CCT reveals the asymmetric folding conformation of a type II chaperonin. Nat. Struct. Biol. *6*, 639–642.

Lupas, A. (1996). Coiled coils: new structures and new functions. Trends Biochem. Sci. *21*, 375–382.

Mayhew, M., da Silva, A.C., Martin, J., Erdjument-Bromage, H., Tempst, P., and Hartl, F.U. (1996). Protein folding in the central cavity of the GroEL-GroES chaperonin complex. Nature *379*, 420–426.

Miller, S., Lesk, A.M., Janin, J., and Chothia, C. (1987). The accessible surface area and stability of oligomeric proteins. Nature *328*, 834–836.

Nelson, R.J., Ziegelhoffer, T., Nicolet, C., Werner-Washburne, M., and Craig, E.A. (1992). The translation machinery and 70 kd heat shock protein cooperate in protein synthesis. Cell *71*, 97–105.

Nicholls, A., Bharadwaj, R., and Honig, B. (1993). Grasp - Graphical Representation and Analysis of Surface-Properties. Biophysical J. *64*, A166–A166.

Otwinowski, Z., and Minor, W. (1997). Processing of X-ray diffraction data collected in oscillation mode. Methods Enzymol. *276*, 307–326.

Perrakis, A., Morris, R., and Lamzin, V.S. (1999). Automated protein model building combined with iterative structure refinement. Nat. Struct. Biol. *6*, 458–463.

Roseman, A.M., Chen, S., White, H., Braig, K., and Saibil, H.R. (1996). The chaperonin ATPase cycle: mechanism of allosteric switching and movements of substrate-binding domains in GroEL. Cell *87*, 241–251.

Roseman, M.A. (1988). Hydrophobicity of polar amino acid side chains is markedly reduced by flanking peptide bonds. J. Mol. Biol. *200*, 513–522.

Rüdiger, S., Germeroth, L., Schneider-Mergener, J., and Bukau, B. (1997). Substrate specificity of the DnaK chaperone determined by screening cellulose-bound peptide libraries. Embo. J. *16*, 1501–1507.

Saibil, H. (2000). Molecular chaperones: containers and surfaces for folding, stabilising or unfolding proteins. Curr. Opin. Struct. Biol. *10*, 251–258.

Scheufler, C., Brinker, A., Bourenkov, G., Pegoraro, S., Moroder, L., Bartunik, H., Hartl, F.U., and Moarefi, I. (2000). Structure of TPR domain-peptide complexes: critical elements in the assembly of the Hsp70-Hsp90 multichaperone machine. Cell *101*, 199–210.

Schoehn, G., Quaite-Randall, E., Jimenez, J.L., Joachimiak, A., and Saibil, H.R. (2000). Three conformations of an archaeal chaperonin, TF55 from Sulfolobus shibatae. J. Mol. Biol. *296*, 813–819.

Schröder, H., Langer, T., Hartl, F.U., and Bukau, B. (1993). DnaK,

DnaJ and GrpE form a cellular chaperone machinery capable of repairing heat-induced protein damage. Embo. J. *12*, 4137–4144.

Shtilerman, M., Lorimer, G.H., and Englander, S.W. (1999). Chaperonin function: folding by forced unfolding. Science *284*, 822–825.

Siegers, K., Waldmann, T., Leroux, M.R., Grein, K., Shevchenko, A., Schiebel, E., and Hartl, F.U. (1999). Compartmentation of protein folding in vivo: sequestration of non-native polypeptide by the chaperonin-GimC system. Embo. J. *18*, 75–84.

Sigler, P.B., Xu, Z., Rye, H.S., Burston, S.G., Fenton, W.A., and Horwich, A.L. (1998). Structure and function in GroEL-mediated protein folding. Annu. Rev. Biochem. *67*, 581–608.

Terwilliger, T.C., and Berendzen, J. (1999). Automated MAD and MIR structure solution. Acta Crystallogr. Sect. D. Biol. Crystallogr. *55*, 849–861.

Teter, S.A., Houry, W.A., Ang, D., Tradler, T., Rockabrand, D., Fischer, G., Blum, P., Georgopoulos, C., and Hartl, F.U. (1999). Polypeptide flux through bacterial Hsp70: DnaK cooperates with trigger factor in chaperoning nascent chains. Cell *97*, 755–765.

Thulasiraman, V., Yang, C.F., and Frydman, J. (1999). In vivo newly translated polypeptides are sequestered in a protected folding environment. Embo. J. *18*, 85–95.

Vainberg, I.E., Lewis, S.A., Rommelaere, H., Ampe, C., Vandekerckhove, J., Klein, H.L., and Cowan, N.J. (1998). Prefoldin, a chaperone that delivers unfolded proteins to cytosolic chaperonin. Cell *93*, 863–873.

Weissman, J.S., Rye, H.S., Fenton, W.A., Beechem, J.M., and Horwich, A.L. (1996). Characterization of the active intermediate of a GroEL-GroES-mediated protein folding reaction. Cell *84*, 481–490.

Xu, Z., Horwich, A.L., and Sigler, P.B. (1997). The crystal structure of the asymmetric GroEL-GroES-(ADP)7 chaperonin complex. Nature *388*, 741–750.

Yaffe, M.B., Farr, G.W., Miklos, D., Horwich, A.L., Sternlicht, M.L., and Sternlicht, H. (1992). TCP1 complex is a molecular chaperone in tubulin biogenesis. Nature *358*, 245–248.

Zhu, X., Zhao, X., Burkholder, W.F., Gragerov, A., Ogata, C.M., Gottesman, M.E., and Hendrickson, W.A. (1996). Structural analysis of substrate binding by the molecular chaperone DnaK. Science *272*, 1606–1614.

Protein Data Bank ID Code

Coordinates have been desposited in the Protein Data Bank under ID code 1FXK.